Evidence for the decay $B^0 \to J/\psi \omega$ and measurement of the relative branching fractions of B^0_s meson decays to $J/\psi \eta$ and $J/\psi \eta'$ ☆

LHCb Collaboration

Abstract

First evidence of the $B^0 \to J/\psi \omega$ decay is found and the $B^0_s \to J/\psi \eta$ and $B^0_s \to J/\psi \eta'$ decays are studied using a dataset corresponding to an integrated luminosity of $1.0\ \text{fb}^{-1}$ collected by the LHCb experiment in proton–proton collisions at a centre-of-mass energy of $\sqrt{s} = 7$ TeV. The branching fractions of these decays are measured relative to that of the $B^0 \to J/\psi \rho^0$ decay:

$$\frac{\mathcal{B}(B^0 \to J/\psi \omega)}{\mathcal{B}(B^0 \to J/\psi \rho^0)} = 0.89 \pm 0.19(\text{stat})^{+0.07}_{-0.13}(\text{syst}),$$

$$\frac{\mathcal{B}(B^0_s \to J/\psi \eta)}{\mathcal{B}(B^0 \to J/\psi \rho^0)} = 14.0 \pm 1.2(\text{stat})^{+1.1}_{-1.5}(\text{syst})^{+1.1}_{-1.0}\left(\frac{f_d}{f_s}\right),$$

$$\frac{\mathcal{B}(B^0_s \to J/\psi \eta')}{\mathcal{B}(B^0 \to J/\psi \rho^0)} = 12.7 \pm 1.1(\text{stat})^{+0.5}_{-1.3}(\text{syst})^{+1.0}_{-0.9}\left(\frac{f_d}{f_s}\right),$$

where the last uncertainty is due to the knowledge of f_d/f_s, the ratio of b-quark hadronization factors that accounts for the different production rate of B^0 and B^0_s mesons. The ratio of the branching fractions of $B^0_s \to J/\psi \eta'$ and $B^0_s \to J/\psi \eta$ decays is measured to be

$$\frac{\mathcal{B}(B^0_s \to J/\psi \eta')}{\mathcal{B}(B^0_s \to J/\psi \eta)} = 0.90 \pm 0.09(\text{stat})^{+0.06}_{-0.02}(\text{syst}).$$

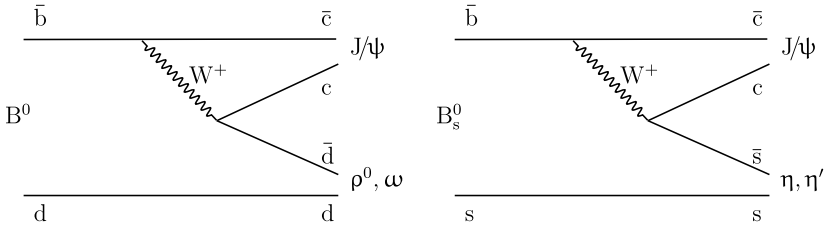© 2012 CERN. Published by Elsevier B.V. All rights reserved.

Fig. 1. Examples of the dominant diagrams for the $B^0_{(s)} \to J/\psi X^0$ decays (where $X^0 = \eta, \eta', \omega$ or ρ^0).

1. Introduction

Decays of B mesons into a J/ψ and a light meson are dominated by color-suppressed tree diagrams involving $\bar{b} \to \bar{c}c\bar{s}$ and $\bar{b} \to \bar{c}c\bar{d}$ transitions (see Fig. 1). Contributions from other diagrams are expected to be small [1]. Measurements of the branching fractions of these decays can help to shed light on hadronic interactions. The decay $B^0 \to J/\psi\omega$ has not been observed previously. The CLEO Collaboration has set the most restrictive upper limit to date of $\mathcal{B}(B^0 \to J/\psi\omega) < 2.7 \times 10^{-4}$ at 90% confidence level [2].

The $B^0_s \to J/\psi\eta^{(\prime)}$ decays were observed by the Belle Collaboration [3] with branching fractions $\mathcal{B}(B^0_s \to J/\psi\eta) = (5.10 \pm 0.50 \pm 0.25^{+1.14}_{-0.79}) \times 10^{-4}$ and $\mathcal{B}(B^0_s \to J/\psi\eta') = (3.71 \pm 0.61 \pm 0.18^{+0.83}_{-0.57}) \times 10^{-4}$, where the first uncertainty is statistical, the second is systematic and the third one is due to an uncertainty of the number of produced $B^0_s\bar{B}^0_s$ pairs. Since both final states are *CP* eigenstates, time-dependent *CP* violation studies and access to the B^0_s–$\bar{B}^0_s$ mixing phase ϕ_s will be possible in the future [4,5]. The theoretical prediction for these branching fractions and their ratio relies on knowledge of the η–η' mixing phase ϕ_P. Taking $\phi_P = (41.4 \pm 0.5)°$ [6] and ignoring a possible gluonic component and corrections due to form factors, the ratio becomes

$$\frac{\mathcal{B}(B^0_s \to J/\psi\eta')}{\mathcal{B}(B^0_s \to J/\psi\eta)} \times \frac{\mathcal{F}^\eta_s}{\mathcal{F}^{\eta'}_s} = \frac{1}{\tan^2 \phi_P} = 1.28^{+0.10}_{-0.08}.$$

Here $\mathcal{F}^{\eta^{(\prime)}}_s$ is the phase space factor of the $B^0_s \to J/\psi\eta^{(\prime)}$ decay and the uncertainty is due to the inaccuracy in the knowledge of the mixing phase. As discussed in Ref. [1], a precise measurement of this ratio tests $SU(3)$ flavour symmetry. In addition, in combination with other measurements, the fraction of the gluonic component in the η' meson can eventually be estimated [7].

The analysis presented here is based on a data sample corresponding to an integrated luminosity of 1.0 fb^{-1} collected by the LHCb detector in 2011 in pp collisions at a centre-of-mass energy of $\sqrt{s} = 7$ TeV. The branching fractions of these decays are measured relative to $\mathcal{B}(B^0 \to J/\psi\rho^0)$ and the ratio $\frac{\mathcal{B}(B^0_s \to J/\psi\eta')}{\mathcal{B}(B^0_s \to J/\psi\eta)}$ is determined.

2. LHCb detector

The LHCb detector [8] is a single-arm forward spectrometer covering the pseudorapidity range $2 < \eta < 5$, designed for the study of b- and c-hadrons. The detector includes a high precision tracking system consisting of a silicon-strip vertex detector surrounding the pp interaction region, a large-area silicon-strip detector located upstream of a dipole magnet with a bending power of about 4 T m, and three stations of silicon-strip detectors and straw drift tubes placed

downstream. The combined tracking system has a momentum resolution $\Delta p/p$ that varies from 0.4% at 5 GeV/c to 0.6% at 100 GeV/c, and an impact parameter resolution of 20 μm for tracks with high transverse momentum (p_T). Charged hadrons are identified using two ring-imaging Cherenkov (RICH) detectors. Photon, electron and hadron candidates are identified by a calorimeter system consisting of scintillating-pad and pre-shower detectors, and electromagnetic and hadron calorimeters. Muons are identified by a system composed of alternating layers of iron and multiwire proportional chambers.

The trigger consists of a hardware stage, based on information from the calorimeter and muon systems, followed by a software stage which applies a full event reconstruction. This analysis uses events triggered by one or two muon candidates. In the case of one muon, the hardware level requirement was for its p_T to be larger than 1.5 GeV/c; in case of two muons the restriction $\sqrt{p_{T_1} \cdot p_{T_2}} > 1.3$ GeV/c was applied. At the software level, the two muons were required to have an invariant mass in the interval $2.97 < m_{\mu^+\mu^-} < 3.21$ GeV/c^2 and to be consistent with originating from the same vertex. To avoid the possibility that a few events with high occupancy dominate the trigger processing time, a set of global event selection requirements based on hit multiplicities was applied.

For the simulation, pp collisions are generated using PYTHIA 6.4 [9] with a specific LHCb configuration [10]. Decays of hadronic particles are described by EVTGEN [11] in which final state radiation is generated using PHOTOS [12]. The interaction of the generated particles with the detector and its response are implemented using the GEANT4 toolkit [13] as described in Ref. [14]. The digitized output is passed through a full simulation of both the hardware and software trigger and then reconstructed in the same way as the data.

3. Data sample and common selection requirements

The decays $B^0_{(s)} \to J/\psi X^0$ (where $X^0 = \eta$, η', ω and $\pi^+\pi^-$) are reconstructed using the $J/\psi \to \mu^+\mu^-$ decay mode. The X^0 candidates are reconstructed in the $\eta \to \gamma\gamma$, $\eta \to \pi^+\pi^-\pi^0$, $\eta' \to \rho^0\gamma$, $\eta' \to \eta\pi^+\pi^-$ and $\omega \to \pi^+\pi^-\pi^0$ final states. Pairs of oppositely charged particles identified as muons, each having $p_T > 550$ MeV/c and originating from a common vertex, are combined to form $J/\psi \to \mu^+\mu^-$ candidates. Well identified muons are selected by requiring that the difference in logarithms of the global likelihood of the muon hypothesis, $\Delta \ln \mathcal{L}_{\mu h}$, provided by the particle identification detectors [15], with respect to the hadron hypothesis is greater than zero. The fit of the common two-prong vertex is required to satisfy $\chi^2/\mathrm{ndf} < 20$, where ndf is the number of degrees of freedom. The vertex is deemed to be well separated from the reconstructed primary vertex of the pp interaction by requiring the decay length significance to be greater than 3. Finally, the invariant mass of the dimuon combination is required to be within ± 40 MeV/c^2 of the nominal J/ψ mass [16].

To identify charged pions the difference between the logarithmic likelihoods of the pion and kaon hypotheses provided by RICH detectors, $\Delta \ln \mathcal{L}_{\pi K}$, should be greater than zero. In the reconstruction of the $B^0_{(s)} \to J/\psi \pi^+\pi^-$ decay this requirement is tightened to be $\Delta \ln \mathcal{L}_{\pi K} > 2$ so as to suppress the contamination from $B^0_{(s)} \to J/\psi \pi K$ decays with misidentified kaons. In addition, the pion tracks are required to have $p_T > 250$ MeV/c. A minimal value of $\Delta \chi^2_{IP}$, defined as the difference between the χ^2 of the primary vertex, reconstructed with and without the considered track, is required to be larger than four.

Photons are selected from neutral clusters in the electromagnetic calorimeter with minimal transverse energy in excess of 300 MeV. To suppress the large combinatorial background from
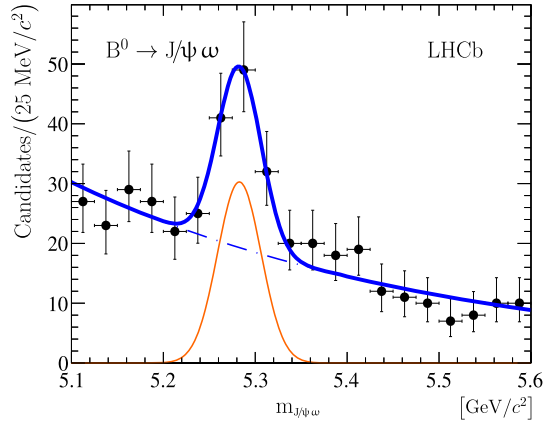
Fig. 2. Invariant mass distribution for selected $B^0 \to J/\psi\omega$ candidates. The black dots correspond to the data distribution, the thick solid blue line is the total fit function, the blue dashed line shows the background contribution and the orange thin line is the signal component of the fit function. (For interpretation of the references to color in this figure legend, the reader is referred to the web version of this article.)

$\pi^0 \to \gamma\gamma$ decays, photons that can form part of a $\pi^0 \to \gamma\gamma$ candidate with invariant mass within ± 25 MeV/c^2 of the nominal π^0 mass are not used for reconstruction of $\eta \to \gamma\gamma$ and $\eta' \to \rho^0\gamma$ candidates.

The $\eta \to \gamma\gamma$ ($\pi^0 \to \gamma\gamma$) candidates are reconstructed as diphoton combinations with invariant mass within $\pm 70(25)$ MeV/c^2 around the nominal $\eta(\pi^0)$ mass. To suppress the combinatorial background to the $\eta \to \gamma\gamma$ decay, the cosine of the decay angle θ_η^*, between the photon momentum in the η rest frame and the direction of the Lorentz boost from the laboratory frame to the η rest frame, is required to have $|\cos\theta_\eta^*| < 0.8$.

The η' candidates are reconstructed as $\eta\pi^+\pi^-$ and $\rho^0\gamma$ combinations with invariant mass within ± 60 MeV/c^2 from the nominal η' mass. For the $\eta' \to \rho^0\gamma$ case, the invariant mass of the $\pi^+\pi^-$ combination is required to be within ± 150 MeV/c^2 of the ρ^0 mass. For $\eta \to \pi^+\pi^-\pi^0$ ($\omega \to \pi^+\pi^-\pi^0$) candidates the invariant mass is required to be within ± 50 MeV/c^2 of the nominal $\eta(\omega)$ mass.

The $B^0_{(s)}$ candidates are formed from $J/\psi X^0$ pairs with $p_T > 3$ GeV/c for the X^0. To improve the invariant mass resolution a kinematic fit [17] is applied. In this fit, constraints are applied on the known masses [16] of intermediate resonances, except the wide ρ^0 and ω states, and it is also required that the candidate's momentum vector points to the associated primary vertex. The χ^2 per degree of freedom for this fit is required to be less than five. Finally, the decay time (cτ) of the $B^0_{(s)}$ candidates is required to be in excess of 150 µm.

4. Evidence for the $B^0 \to J/\psi\omega$ decay

The invariant mass distribution of the selected $J/\psi\omega$ candidates is shown in Fig. 2, where a B^0 signal is visible. To determine the signal yield, an unbinned maximum likelihood fit is performed to this distribution. The signal is modelled by a Gaussian distribution and the background by an exponential function. The peak position is found to be 5284 ± 5 MeV/c^2, which is consistent with the nominal B^0 mass [16] and the resolution is in good agreement with the prediction from simulation. The event yield is determined to be $\mathcal{Y}_{B^0} = 72 \pm 15$.
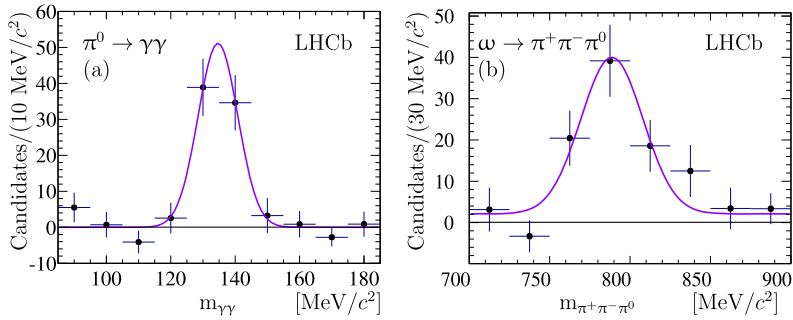
Fig. 3. Background-subtracted (a) $\gamma\gamma$ and (b) $\pi^+\pi^-\pi^0$ invariant mass distributions for $B^0 \to J/\psi\pi^+\pi^-\gamma\gamma$ decays. In both distributions the line is the result of the fit described in the text.

The statistical significance for the observed signal is determined as $\mathcal{S} = \sqrt{-2\ln(\mathcal{L}_\mathcal{B}/\mathcal{L}_{\mathcal{S}+\mathcal{B}})}$, where $\mathcal{L}_{\mathcal{S}+\mathcal{B}}$ and $\mathcal{L}_\mathcal{B}$ denote the likelihood of the signal plus background hypothesis and the background hypothesis, respectively. The statistical significance of the signal is found to be 5.0 standard deviations. Taking into account the systematic uncertainty related to the fit function, which is discussed in detail in Section 7.1, the significance is 4.6σ; this also takes into account the freedom in the peak position and width in the nominal fit.

To demonstrate that the signal originates from $B^0 \to J/\psi\omega$ decays, the sPlot technique [18] has been applied. Using the $J/\psi\pi^+\pi^-\gamma\gamma$ invariant mass as the discriminating variable, the distributions for the invariant masses of the intermediate resonances $\pi^0 \to \gamma\gamma$ and $\omega \to \pi^+\pi^-\pi^0$ have been obtained. The invariant mass window for each corresponding resonance is released and the mass constraint is removed.

The invariant mass distributions for $\gamma\gamma$ and $\pi^+\pi^-\pi^0$ from $B^0 \to J/\psi\omega$ candidates are shown in Fig. 3. Clear signals are seen for both the $\omega \to \pi^+\pi^-\pi^0$ and $\pi^0 \to \gamma\gamma$ decays. The $\gamma\gamma$ distribution is described by a sum of a Gaussian function and a constant. The $\omega \to \pi^+\pi^-\pi^0$ signal is modelled by a convolution of a Gaussian and a Breit–Wigner function with a constant background. The peak positions are in good agreement with the nominal π^0 and ω masses and the yields determined from the fits are compatible with the $B^0 \to J/\psi\omega$ yield. The nonresonant contribution in each case is found to be consistent with zero.

5. Decays into $J/\psi\eta^{(\prime)}$ final states

The invariant mass spectra for $B_s^0 \to J/\psi\eta^{(\prime)}$ candidates are shown in Fig. 4, where signals are visible. To determine the signal yields, unbinned maximum likelihood fits are performed. For all modes apart from $J/\psi\eta^\prime$ ($\eta^\prime \to \rho^0\gamma$), the B_s^0 signal is modelled by a single Gaussian function. In all cases there is a possible corresponding B^0 signal, which is included in the fit model as an additional Gaussian component. The difference of the means of the two Gaussians is fixed to the known difference between the B_s^0 and the B^0 masses [19]. Simulation studies for the $J/\psi\eta^\prime$ ($\eta^\prime \to \rho^0\gamma$) mode indicate that in this case a double Gaussian resolution model is more appropriate. The mean values of the two Gaussian functions are required to be the same, and the ratio of their resolutions and the fraction of the event yield carried by each of the Gaussian functions are fixed at the values obtained from simulation.

The combinatorial background is modelled by an exponential function. In addition, a component is added to describe the contribution from partially reconstructed B decays. It is described with the phase space function for two particles in a three body decay under the hypothesis of
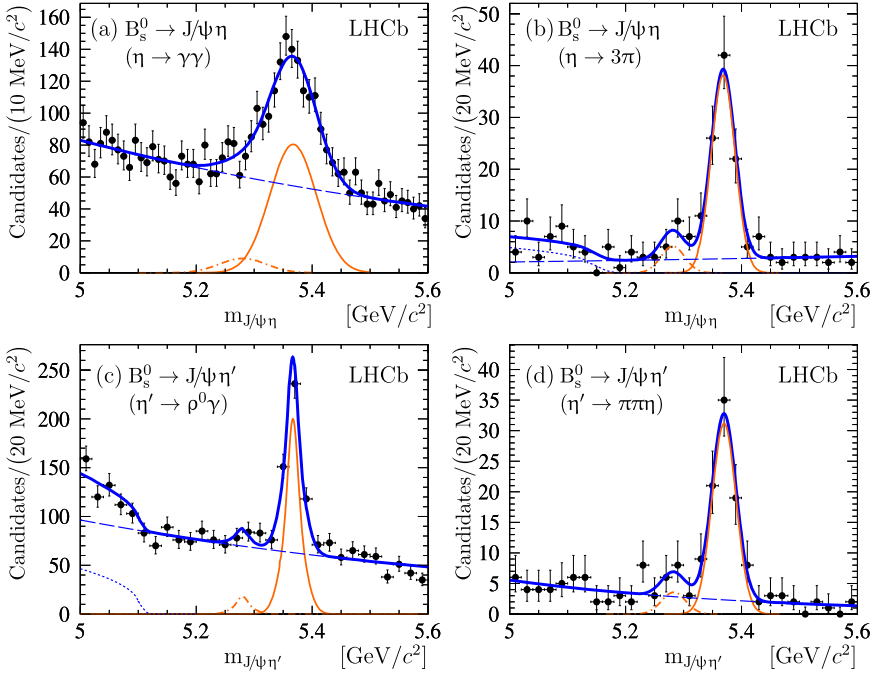
Fig. 4. Invariant mass distributions for selected $B_s^0 \to J/\psi \eta^{(\prime)}$ candidates: (a) $B_s^0 \to J/\psi \eta$ ($\eta \to \gamma\gamma$), (b) $B_s^0 \to J/\psi \eta$ ($\eta \to \pi^+\pi^-\pi^0$), (c) $B_s^0 \to J/\psi \eta'$ ($\eta' \to \rho^0\gamma$) and (d) $B_s^0 \to J/\psi \eta'$ ($\eta' \to \pi^+\pi^-\eta$). In all distributions the black dots show the data. The thin solid orange lines show the signal B_s^0 contributions and the orange dot-dashed lines correspond to the B^0 contributions. The blue dashed lines show the combinatorial background contributions and the dotted blue lines show the partially reconstructed background components. The total fit functions are drawn as solid blue lines. The results of the fit are described in the text. (For interpretation of the references to color in this figure legend, the reader is referred to the web version of this article.)

Table 1
Signal yields, $\mathcal{Y}_{B_s^0}$, the fitted B_s^0 mass, $m_{B_s^0}$ and mass resolutions, $\sigma_{B_s^0}$ for the $B_s^0 \to J/\psi \eta^{(\prime)}$ decays.

Mode	$\mathcal{Y}_{B_s^0}$	$m_{B_s^0}$ [MeV/c^2]	$\sigma_{B_s^0}$ [MeV/c^2]
$B_s^0 \to J/\psi \eta$ ($\eta \to \gamma\gamma$)	810 ± 65	5367.2 ± 3.5	40.1 ± 3.6
$B_s^0 \to J/\psi \eta$ ($\eta \to \pi^+\pi^-\pi^0$)	94 ± 11	5368.4 ± 2.6	20.3 ± 2.3
$B_s^0 \to J/\psi \eta'$ ($\eta' \to \rho^0\gamma$)	336 ± 30	5367.0 ± 1.1	8.0 ± 1.1
$B_s^0 \to J/\psi \eta'$ ($\eta' \to \pi^+\pi^-\eta$)	79 ± 10	5369.0 ± 2.8	20.7 ± 2.3

$B \to J/\psi \eta^{(\prime)} X$ decay, where X can be either a kaon or a pion, which escapes detection. The phase space function is convolved with a resolution factor, which is fixed at the value of the signal resolution.

The fit results are summarized in Table 1. In all cases the position of the signal peak is consistent with the nominal B_s^0 mass [16] and the resolutions agree with the expectations from simulation. The statistical significances of all the B_s^0 decays exceed 7σ.

To test the resonance structure of the $B_s^0 \to J/\psi \eta^{(\prime)}$ decays, the sPlot technique is used. For the π^0, η and η' candidates the background-subtracted invariant mass distributions are studied. The restrictions on the invariant mass for the corresponding resonance are released and the mass
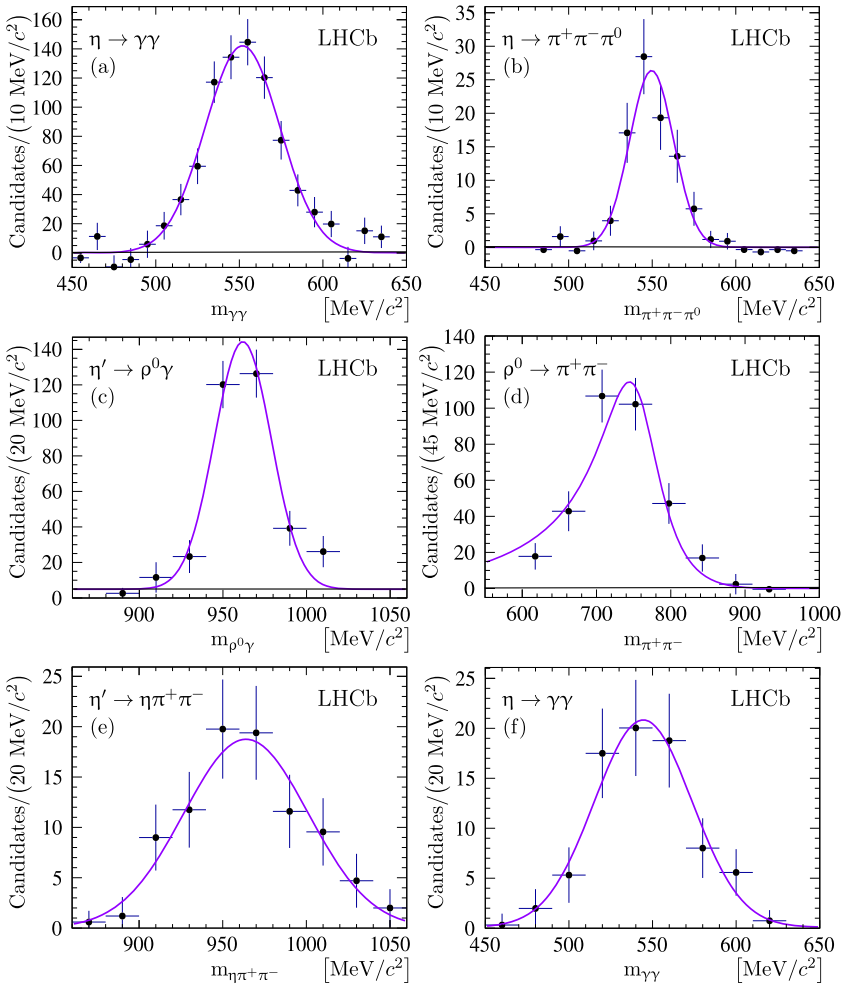
Fig. 5. Background-subtracted invariant mass distributions for (a) $\gamma\gamma$ from $B_s^0 \to J/\psi\eta$ ($\eta \to \gamma\gamma$); (b) $\pi^+\pi^-\pi^0$ from $B_s^0 \to J/\psi\eta$ ($\eta \to \pi^+\pi^-\pi^0$); (c) and (d) $\pi^+\pi^-\gamma$ and $\pi^+\pi^-$ from $B_s^0 \to J/\psi\eta'$ ($\eta' \to \rho^0\gamma$, $\rho \to \pi^+\pi^-$); (e) and (f) $\eta\pi^+\pi^-$ and $\gamma\gamma$ from $B_s^0 \to J/\psi\eta'$ ($\eta' \to \eta\pi^+\pi^-$). The purple line is the result of the fit described in the text. (For interpretation of the references to color in this figure legend, the reader is referred to the web version of this article.)

constraints (if any) removed. The background-subtracted distributions are then fitted with the sum of a Gaussian function and a constant component for the resonant and nonresonant components respectively. In the fit of the dipion invariant mass for the $\eta' \to \pi^+\pi^-\gamma$ decay a modified relativistic Breit–Wigner function is used as the signal component [20,21].

Background-subtracted invariant mass distributions of the intermediate resonance states from the $B_s^0 \to J/\psi X^0$ decays, are shown in Fig. 5. Clear signals are seen. In all cases the signal yields determined from the fits are in agreement with the event yield in the B_s^0 signal within one standard deviation (Table 1). The signal positions are consistent with the nominal masses of the $\eta^{(\prime)}$ mesons and the nonresonant contribution appears to be negligible. In each case the invariant mass resolution agrees with the expectation from simulation studies.
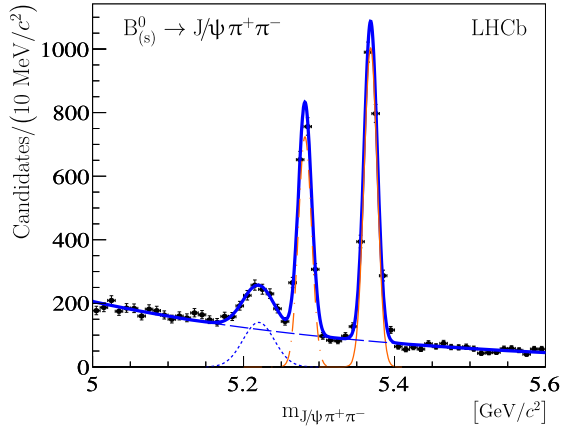
Fig. 6. Invariant mass distribution for selected $B^0_{(s)} \to J/\psi \pi^+\pi^-$ candidates. The black dots show the data. The dot-dashed thin orange line shows the signal B^0 contribution and the orange solid line shows the signal B^0_s contribution, a reflection from misidentified $B^0 \to J/\psi$ ($K^* \to K\pi$) is shown by a blue dotted line. The blue dashed line shows the background contribution. The total fit function is shown as a solid blue line. (For interpretation of the references to color in this figure legend, the reader is referred to the web version of this article.)

6. The $B^0 \to J/\psi \pi^+\pi^-$ decay

The $B^0 \to J/\psi \rho^0$ ($\rho^0 \to \pi^+\pi^-$) decay is used as a normalization channel [22]. Since it contains a J/ψ meson and two pions in the final state, the systematic uncertainty is reduced in the ratio of the branching fractions, as the corresponding reconstruction and particle identification uncertainties are expected to cancel.

The invariant mass spectrum for $B^0_{(s)} \to J/\psi \pi^+\pi^-$ candidates is presented in Fig. 6, where three clear signals are visible. Two narrow signals correspond to the $B^0 \to J/\psi \pi^+\pi^-$ and $B^0_s \to J/\psi \pi^+\pi^-$ decays. The latter decay has been studied in detail in Refs. [23,24]. The peak at lower mass corresponds to contamination from $B^0 \to J/\psi K^{*0}$ ($K^{*0} \to K^+\pi^-$) decays with a kaon being misreconstructed as a pion. A contribution from $B^0_s \to J/\psi K^{*0}$ decay is considered to be negligible.

The invariant mass distribution is fitted with a sum of three Gaussian functions to describe the three signals, and an exponential function to represent the background. The fit gives a yield of 1143 ± 39 for $B^0 \to J/\psi \pi^+\pi^-$.

Previous studies at BaBar [22] show that the $B^0 \to J/\psi \pi^+\pi^-$ final state has contributions from decays of ρ^0 and K^0_S mesons, as well as a broad S-wave component. A further component from the $f_2(1270)$ resonance is also hinted at in the BaBar study. To study the dipion mass distribution the sPlot technique is used. With the $J/\psi \pi^+\pi^-$ invariant mass as the discriminating variable, the $\pi^+\pi^-$ invariant mass spectrum from $B^0 \to J/\psi \pi^+\pi^-$ decays is obtained (see Fig. 7). A dominant ρ^0 signal is observed together with a narrow peak around 498 MeV/c^2 due to K^0_S decays. There is also a wide enhancement at a mass close to 1260 MeV/c^2. The position and width of this structure are consistent with the interpretation as a contribution from the $f_2(1270)$ state. This will be the subject of a future publication.

The distribution is fitted with the sum of several components. A P-wave modified relativistic Breit–Wigner function [20,21] multiplied by a phase space factor describes the ρ^0 signal. A D-wave relativistic Breit–Wigner function is added to describe the enhancement at
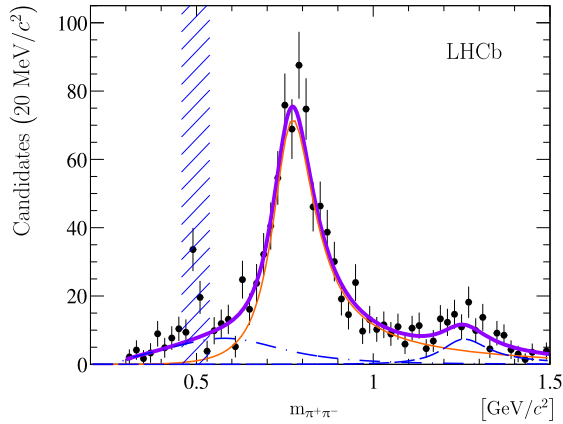
Fig. 7. Background-subtracted $\pi^+\pi^-$ invariant mass distribution from $B^0 \to J/\psi\pi^+\pi^-$ decays. The black dots show the data. A violet solid line denotes the total fit function, the solid orange line shows the ρ^0 signal contribution and the blue dashed line shows the $f_2(1270)$ contribution. The blue dot-dashed line shows the contribution from the $f_0(500)$. The region ± 40 MeV/c^2 around the K_S^0 mass is excluded from the fit.

Table 2
Fitted yields of the ρ^0 resonance, the relative yields of the $f_2(1270)$ and $f_0(500)$ components and probabilities, $\mathcal{P}$, of the fits to the uncorrected and efficiency-corrected $\pi^+\pi^-$ invariant mass distributions.

	Uncorrected fit	Efficiency-corrected fit
ρ^0 event yield	811 ± 38	$(27.6 \pm 1.3) \times 10^3$
$f_0(500)$ fraction	0.20 ± 0.04	0.19 ± 0.04
$f_2(1270)$ fraction	0.14 ± 0.03	0.16 ± 0.04
$\mathcal{P}$ [%]	40	46

1260 MeV/c^2. The parameters (width and mean value) of this function are fixed to the known $f_2(1270)$ mass and decay width [16]. The S-wave contribution expected from the $f_0(500)$ resonance is modelled by a Zou and Bugg [25,26] function with parameters from Ref. [27]. The ρ^0 parameters (mass and width) are fixed at their nominal values and the region around the K_S^0 peak is excluded from the fit. The excluded region is ± 40 MeV/c^2 which is four times the mass resolution. A small systematic uncertainty is induced by neglecting the ρ^0–ω interference. The value of the uncertainty is estimated to be 0.5% relative to the ρ^0 event yield.

The reconstruction and selection efficiency for the dipion system has some dependence on the dipion invariant mass. A study using simulated data has shown that with the increase of the $\pi^+\pi^-$ invariant mass in the range 300–1500 MeV/c^2 the efficiency decreases by approximately 16%. As the ρ^0 meson has a significant width, this dependence needs to be accounted for in the determination of the ρ^0 signal yield. For this, the efficiency dependence on $\pi^+\pi^-$ invariant mass extracted from the simulation is described with a linear function. Then each entry in the invariant mass distribution is given a weight proportional to the inverse value of the efficiency function and the efficiency-corrected invariant mass distribution is refitted with the same sum of functions to extract the efficiency-corrected event yield for $B^0 \to J/\psi\rho^0$. The resulting fit parameters both for the uncorrected and efficiency-corrected distributions are listed in Table 2.

Table 3

Branching fractions of the intermediate resonances, total efficiencies (excluding the branching fractions of the intermediate resonances), $\varepsilon^{\mathrm{tot}}$, and the photon and π^0 efficiency correction factors η^{corr} for various channels. For the $B^0 \to J/\psi \rho^0$ decay the total efficiency includes only the detector acceptance and trigger efficiencies, as the reconstruction and selection efficiency for this channel has been discussed in Section 6.

Mode	$\mathcal{B}$ [%]	$\varepsilon^{\mathrm{tot}}$ [%]	η^{corr} [%]
$B_s^0 \to J/\psi\eta\ (\eta \to \gamma\gamma)$	39.31 ± 0.20	0.236 ± 0.006	98.0 ± 7.5
$B_s^0 \to J/\psi\eta\ (\eta \to \pi^+\pi^-\pi^0)$	22.74 ± 0.28	0.059 ± 0.002	94.1 ± 7.5
$B_s^0 \to J/\psi\eta'\ (\eta' \to \rho^0\gamma)$	29.3 ± 0.6	0.142 ± 0.004	98.0 ± 3.7
$B_s^0 \to J/\psi\eta'\ (\eta' \to \pi^+\pi^-\eta)$	18.6 ± 0.3	0.068 ± 0.003	96.0 ± 7.5
$B^0 \to J/\psi\omega\ (\omega \to \pi^+\pi^-\pi^0)$	89.2 ± 0.7	0.043 ± 0.002	94.1 ± 7.5
$B^0 \to J/\psi\rho^0\ (\rho^0 \to \pi^+\pi^-)$	98.90 ± 0.16	12.6 ± 0.5	–

7. Measurements of ratios of branching fractions

Ratios of branching fractions are measured using the formula

$$\mathcal{R}_{\mathrm{B,Y^0}}^{\mathrm{B,X^0}} \equiv \frac{\mathcal{B}(\mathrm{B} \to J/\psi X^0)}{\mathcal{B}(\mathrm{B} \to J/\psi Y^0)} = \frac{\mathcal{Y}(\mathrm{B} \to J/\psi X^0)}{\mathcal{Y}(\mathrm{B} \to J/\psi Y^0)} \times \frac{\mathcal{B}_{Y^0}}{\mathcal{B}_{X^0}} \times \frac{\varepsilon^{\mathrm{tot}}_{\mathrm{B} \to J/\psi Y^0}}{\varepsilon^{\mathrm{tot}}_{\mathrm{B} \to J/\psi X^0}},$$

where $\mathcal{Y}$ are the measured event yields, $\varepsilon^{\mathrm{tot}}$ are the total efficiencies, excluding the branching fractions of light mesons and $\mathcal{B}_{X^0}(\mathcal{B}_{Y^0})$ is the relevant branching ratio of the light meson $X^0(Y^0)$ to the final state under consideration [16]. In cases where decays of different types of B mesons are compared, the ratio of the branching fractions is multiplied by the ratio of the corresponding b-quark hadronization fractions f_d/f_s [28].

The total efficiencies consist of three components: the geometrical acceptance of the detector, the reconstruction and selection efficiency and the trigger efficiency. For the $B^0 \to J/\psi\rho^0$ decay, the event yield $\mathcal{Y}$ implies the value weighted by the selection and reconstruction efficiency from Table 2. Only the acceptance and trigger efficiencies are included in $\varepsilon^{\mathrm{tot}}_{B^0 \to J/\psi\rho^0}$. All efficiency components have been determined using the simulation and the values are listed in Table 3.

For channels with photons and neutral pions in the final states, the reconstruction and selection efficiencies are corrected for the difference in the photon reconstruction between the data and simulation. This correction factor has been determined by comparing the relative yields of the reconstructed $B^+ \to J/\psi K^{*+}\ (K^{*+} \to K^+\pi^0)$ and $B^+ \to J/\psi K^+$ decays. The results of these studies are convolved with the background subtracted photon momentum spectra to give the correction factor for each channel. The values of the correction factors (η^{corr}) are also listed in Table 3.

7.1. Systematic uncertainties

Most systematic uncertainties cancel in the branching fraction ratios, in particular, those related to the muon and J/ψ reconstruction and identification. For the final states with photons the largest systematic uncertainty is related to the efficiency of π^0/γ reconstruction and identification, as described above. The uncertainties of the applied corrections reflect simulation statistics, and are taken as systematic uncertainties on the branching fractions ratios.

Another systematic uncertainty is due to the charged particle reconstruction efficiency which has been studied through a comparison between data and simulation. For the ratios where

Table 4
Relative systematic uncertainties for ratios of the branching fractions ($\mathcal{R}$) for the $B_s^0 \to J/\psi\eta^{(\prime)}$ channels [%].

Parameter	$\mathcal{R}^{\eta\to\gamma\gamma}_{\eta\to\pi^+\pi^-\pi^0}$	$\mathcal{R}^{\eta'\to\eta\pi^+\pi^-}_{\eta\to\gamma\gamma}$	$\mathcal{R}^{\eta'\to\eta\pi^+\pi^-}_{\eta\to\pi^+\pi^-\pi^0}$	$\mathcal{R}^{\eta'\to\rho^0\gamma}_{\eta\to\gamma\gamma}$	$\mathcal{R}^{\eta'\to\rho^0\gamma}_{\eta\to\pi^+\pi^-\pi^0}$	$\mathcal{R}^{\eta'\to\rho^0\gamma}_{\eta'\to\eta\pi^+\pi^-}$
η^{corr}	–	–	–	3.8	3.9	3.9
$\pi^\pm$ reco	2×1.8	2×1.8	–	2×1.8	–	–
Trigger	1.1	1.1	1.1	1.1	1.1	1.1
Fit function	$+3.7$ -0.0	$+9.9$ -0.0	$+1.3$ -5.6	$+3.4$ -0.0	< 0.1	$+0.0$ -2.8
$\mathcal{B}(\eta, \eta', \omega)$	1.3	1.7	2.0	2.1	1.8	2.6

this does not cancel exactly, the corresponding systematic uncertainty is taken to be 1.8% per pion [29].

The systematic uncertainty related to the trigger efficiency has been obtained by comparison of the trigger efficiency ratios in data and simulation for the high yield decay mode $B^\pm \to J/\psi K^\pm$ with similar kinematics and the same trigger requirements [30]. This uncertainty is taken to be 1.1%.

In the ratios where decays of B mesons of different types are compared (B^0 or B_s^0), knowledge of the hadronization fraction ratio f_d/f_s is required. The measured value of this ratio [28] has an asymmetric uncertainty of $^{+7.9}_{-7.5}\%$.

Systematic uncertainties related to the fit model are estimated using a number of alternative models for the description of the invariant mass distributions. For the $B_s^0 \to J/\psi\eta^{(\prime)}$ decays the tested alternatives include a fit without the B^0 component, a fit with the means of the Gaussians fixed to the nominal B meson masses, a fit with the width of the Gaussians fixed to the expected mass resolutions from simulation and substitution of the exponential background hypothesis with first- and second-order polynomials. This uncertainty is calculated for the ratios of the event yields. For each alternative fit model the ratio of the event yields is calculated and the systematic uncertainty is then determined as the maximum deviation of this ratio from the ratio obtained with the baseline model.

A similar study is performed for the $B^0 \to J/\psi\omega$ channel. As the fit with one Gaussian function is the baseline model in this case, here the alternative model is a fit with two Gaussian functions (allowing a possible B_s^0 signal).

In the $B^0 \to J/\psi\rho^0$ case, an alternative model replaces the Zou–Bugg $f_0(500)$ term with a Breit–Wigner shape. The mass and width of the broad $f_0(500)$ state are not well known. The mass measured by various experiments varies in a range between 400 and 1200 MeV/c^2 and the measured width ranges between 600 and 1000 MeV/c^2 [16]. Therefore, the $f_0(500)$ parameters are varied in this range and the ρ^0 yield is determined. Again, the maximum deviation from the baseline model is treated as the systematic uncertainty of the fit.

The uncertainties related to the knowledge of the branching fractions of η, η', π^0 and ω decays are taken from Ref. [16]. Other systematic uncertainties, such as those related to the selection criteria are negligible. The systematic uncertainties are summarized in Tables 4 and 5. The total systematic uncertainties are estimated using a simulation technique (see Section 7.2).

7.2. Results

The final ratios $\mathcal{R}^{B_s^0,\eta'}_{B_s^0,\eta}$, $\mathcal{R}^{B_s^0,\eta^{(\prime)}}_{B^0,\rho^0}$ and $\mathcal{R}^{B^0,\omega}_{B^0,\rho^0}$ are determined using a procedure that combines χ^2-minimization with constraints and simplified simulation. First, the χ^2 is minimized

Table 5
Systematic uncertainties for ratios of the branching fractions ($\mathcal{R}$) relative to $B^0 \to J/\psi \rho^0$ [%].

Parameter	$\mathcal{R}^{B_s^0, \eta \to \gamma\gamma}_{B^0, \rho^0 \to \pi^+\pi^-}$	$\mathcal{R}^{B_s^0, \eta \to \pi^+\pi^-\pi^0}_{B^0, \rho^0 \to \pi^+\pi^-}$	$\mathcal{R}^{B_s^0, \eta' \to \rho^0\gamma}_{B^0, \rho^0 \to \pi^+\pi^-}$	$\mathcal{R}^{B_s^0, \eta' \to \eta\pi^+\pi^-}_{B^0, \rho^0 \to \pi^+\pi^-}$	$\mathcal{R}^{B^0, \omega \to \pi^+\pi^-\pi^0}_{B^0, \rho^0 \to \pi^+\pi^-}$
η^{corr}	7.6	8.0	3.8	7.8	8.0
$\pi^\pm$ reco	2×1.8	–	–	–	–
Trigger	1.1	1.1	1.1	1.1	1.1
Fit function	$+5.1$ -3.7	$+5.0$ -4.3	$+5.0$ -5.7	$+5.0$ -8.7	$+6.4$ -8.8
$\mathcal{B}(\eta, \eta', \omega)$	0.5	1.2	2.1	1.6	0.8

$$\chi^2 = \sum_i \chi_i^2,$$

where the sum is performed over the six measured event yields for the six different modes: $B_s^0 \to J/\psi \eta(\eta \to \gamma\gamma)$, $B_s^0 \to J/\psi \eta(\eta \to \pi^+\pi^-\pi^0)$, $B_s^0 \to J/\psi \eta'(\eta' \to \rho^0\gamma)$, $B_s^0 \to J/\psi \eta'(\eta' \to \eta\pi^+\pi^-)$, $B^0 \to J/\psi \omega$ and $B^0 \to J/\psi \rho^0$, and $\chi_i^2 = \frac{(x - y_i)^2}{\sigma_{y_i}^2}$. In this procedure the following constraints are imposed

$$\frac{\mathcal{Y}_{B_s^0 \to J/\psi \eta(\eta \to \gamma\gamma)}}{\varepsilon_{B_s^0 \to J/\psi \eta(\eta \to \gamma\gamma)} \times \mathcal{B}(\eta \to \gamma\gamma)} = \frac{\mathcal{Y}_{B_s^0 \to J/\psi \eta(\eta \to \pi^+\pi^-\pi^0)}}{\varepsilon_{B_s^0 \to J/\psi \eta(\eta \to \pi^+\pi^-\pi^0)} \times \mathcal{B}(\eta \to \pi^+\pi^-\pi^0)},$$

$$\frac{\mathcal{Y}_{B_s^0 \to J/\psi \eta'(\eta' \to \rho^0\gamma)}}{\varepsilon_{B_s^0 \to J/\psi \eta'(\eta' \to \rho^0\gamma)} \times \mathcal{B}(\eta' \to \rho^0\gamma)} = \frac{\mathcal{Y}_{B_s^0 \to J/\psi \eta'(\eta' \to \eta\pi^+\pi^-)}}{\varepsilon_{B_s^0 \to J/\psi \eta'(\eta' \to \eta\pi^+\pi^-)} \times \mathcal{B}(\eta' \to \eta\pi^+\pi^-)}.$$

The ratios $\mathcal{R}^{B_s^0, \eta'}_{B_s^0, \eta}$, $\mathcal{R}^{B_s^0, \eta^{(\prime)}}_{B^0, \rho^0}$ and $\mathcal{R}^{B^0, \omega}_{B^0, \rho^0}$ are determined using the event yields obtained from the minimization procedure. For this determination the efficiencies ε_i have been varied using a simplified simulation taking into account correlations between the various components where appropriate. As both the χ^2 and the ratios $\mathcal{R}$ depend only on the ratios of efficiencies, systematic uncertainties are minimized. The remaining systematic uncertainties have been taken into account as uncertainties in the efficiency ratios. In total, 10^6 simulated experiments with different settings of ε_i have been performed. The symmetric 68% intervals have been assigned as the systematic uncertainty.

The obtained ratios $\mathcal{R}$ are

$$\mathcal{R}^{B_s^0, \eta'}_{B_s^0, \eta} = 0.90 \pm 0.09^{+0.06}_{-0.02},$$

$$\mathcal{R}^{B_s^0, \eta}_{B^0, \rho^0} = \left(3.75 \pm 0.31^{+0.30}_{-0.40}\right) \times \left(\frac{f_d}{f_s}\right),$$

$$\mathcal{R}^{B_s^0, \eta'}_{B^0, \rho^0} = \left((3.38 \pm 0.30^{+0.14}_{-0.36}\right) \times \left(\frac{f_d}{f_s}\right),$$

$$\mathcal{R}^{B^0, \omega}_{B^0, \rho^0} = 0.89 \pm 0.19^{+0.07}_{-0.13},$$

where the first uncertainty is statistical and the second is systematic.

8. Summary

With 1.0 fb^{-1} of data, collected in 2011 with the LHCb detector, the first evidence for the $B^0 \to J/\psi\omega$ decay has been found, and its branching fraction, normalized to that of the $B^0 \to J/\psi\rho^0$ decay, is measured to be

$$\frac{\mathcal{B}(B^0 \to J/\psi\omega)}{\mathcal{B}(B^0 \to J/\psi\rho^0)} = 0.89 \pm 0.19\text{(stat)}^{+0.07}_{-0.13}\text{(syst)}.$$

Multiplying by the known value of $\mathcal{B}(B^0 \to J/\psi\rho^0) = (2.7 \pm 0.4) \times 10^{-5}$ [22], the absolute value of the branching fraction is

$$\mathcal{B}(B^0 \to J/\psi\omega) = \left(2.41 \pm 0.52\text{(stat)}^{+0.19}_{-0.35}\text{(syst)} \pm 0.36(\mathcal{B}_{B^0 \to J/\psi\rho^0})\right) \times 10^{-5}.$$

Using the same dataset, the ratio of the branching fractions of $B^0_s \to J/\psi\eta$ and $B^0_s \to J/\psi\eta'$ decays has been measured. As each of the decays has been reconstructed in two final states, the resulting ratio has been calculated through an averaging procedure to be

$$\mathcal{R}^{B^0_s,\eta'}_{B^0_s,\eta} = \frac{\mathcal{B}(B^0_s \to J/\psi\eta')}{\mathcal{B}(B^0_s \to J/\psi\eta)} = 0.90 \pm 0.09\text{(stat)}^{+0.06}_{-0.02}\text{(syst)}.$$

This result is consistent with the previous Belle measurement of $\mathcal{R}^{B^0_s,\eta'}_{B^0_s,\eta} = 0.73 \pm 0.14$ [3], but is more precise. Assuming that the contribution from the purely gluonic component is negligible, this ratio corresponds to a value of the η–η' mixing phase of $\phi_P = (45.5^{+1.8}_{-1.5})°$. The branching fractions of the $B^0_s \to J/\psi\eta$ and $B^0_s \to J/\psi\eta'$ decays have been determined by normalization to the $B^0 \to J/\psi\rho^0$ decay branching fraction, and using the known value of $f_s/f_d = 0.267^{+0.021}_{-0.020}$ [28] their ratios are

$$\frac{\mathcal{B}(B^0_s \to J/\psi\eta)}{\mathcal{B}(B^0 \to J/\psi\rho^0)} = 14.0 \pm 1.2\text{(stat)}^{+1.1}_{-1.5}\text{(syst)}^{+1.1}_{-1.0}\left(\frac{f_d}{f_s}\right),$$

$$\frac{\mathcal{B}(B^0_s \to J/\psi\eta')}{\mathcal{B}(B^0 \to J/\psi\rho^0)} = 12.7 \pm 1.1\text{(stat)}^{+0.5}_{-1.3}\text{(syst)}^{+1.0}_{-0.9}\left(\frac{f_d}{f_s}\right).$$

When multiplying by the known value of $\mathcal{B}(B^0 \to J/\psi\rho^0)$, the branching fractions are measured as

$$\mathcal{B}(B^0_s \to J/\psi\eta) = \left(3.79 \pm 0.31\text{(stat)}^{+0.20}_{-0.41}\text{(syst)}^{+0.29}_{-0.27}\left(\frac{f_d}{f_s}\right) \pm 0.56(\mathcal{B}_{B^0 \to J/\psi\rho^0})\right) \times 10^{-4},$$

$$\mathcal{B}\left(B^0_s \to J/\psi\eta'\right) = \left(3.42 \pm 0.30\text{(stat)}^{+0.14}_{-0.35}\text{(syst)}^{+0.26}_{-0.25}\left(\frac{f_d}{f_s}\right) \pm 0.51(\mathcal{B}_{B^0 \to J/\psi\rho^0})\right) \times 10^{-4}.$$

The branching fractions measured here correspond to the time integrated quantities, while theory predictions usually refer to the branching fractions at $t = 0$. Special care needs to be taken when the B^0_s and B^0 decays are compared at the amplitude level, corresponding to the branching ratio at $t = 0$ [31]. Since the $J/\psi\eta^{(')}$ final states are *CP*-eigenstates, the size of this effect can be as large as 10%, and can be corrected for using input from theory or determined from effective lifetime measurements [31]. With a larger dataset such measurements, as well as studies of η–η' mixing and measurements of *CP* asymmetries in the $B^0_s \to J/\psi\eta^{(')}$ modes will be possible.

Acknowledgements

References

[1] R. Fleischer, R. Knegjens, G. Ricciardi, Exploring CP violation and η–η' mixing with the $B^0_{(s,d)} \to J/\psi \eta^{(\prime)}$ systems, Eur. Phys. J. C 71 (2011) 1798, arXiv:1110.5490.
[2] CLEO Collaboration, M. Bishai, et al., Study of $B^0 \to \psi \rho$, Phys. Lett. B 369 (1996) 186.
[3] Belle Collaboration, J. Li, et al., First observations of $B^0_s \to J/\psi \eta$ and $B^0_s \to J/\psi \eta'$, Phys. Rev. Lett. 108 (2012) 181808, arXiv:1202.0103.
[4] M. Jung, Determining weak phases from $B \to J/\psi P$ decays, arXiv:1206.2050.
[5] P. Colangelo, F. De Fazio, W. Wang, Nonleptonic B_s to charmonium decays: analyses in pursuit of determining the weak phase β_s, Phys. Rev. D 83 (2011) 094027, arXiv:1009.4612.
[6] KLOE Collaboration, F. Ambrosino, et al., Measurement of the pseudoscalar mixing angle and η' gluonium content with KLOE detector, Phys. Lett. B 648 (2007) 267, arXiv:hep-ex/0612029.
[7] X. Liu, H.-n. Li, Z.-J. Xiao, Implications on η–η'–glueball mixing from $B_{d/s} \to J/\psi \eta^{(\prime)}$ decays, Phys. Rev. D 86 (2012) 011501, arXiv:1205.1214.
[8] LHCb Collaboration, A.A. Alves Jr., et al., The LHCb detector at the LHC, JINST 3 (2008) S08005.
[9] T. Sjöstrand, S. Mrenna, P. Skands, PYTHIA 6.4 physics and manual, JHEP 0605 (2006) 026, arXiv:hep-ph/0603175.
[10] I. Belyaev, et al., Handling of the generation of primary events in GAUSS, the LHCb simulation framework, Nuclear Science Symposium Conference Record (NSS/MIC) IEEE (2010) 1155.
[11] D.J. Lange, The EvtGen particle decay simulation package, Nucl. Instrum. Meth. A 462 (2001) 152.
[12] P. Golonka, Z. Was, PHOTOS Monte Carlo: a precision tool for QED corrections in Z and W decays, Eur. Phys. J. C 45 (2006) 97, arXiv:hep-ph/0506026.
[13] GEANT4 Collaboration, J. Allison, et al., Geant4 developments and applications, IEEE Trans. Nucl. Sci. 53 (2006) 270;
GEANT4 Collaboration, S. Agostinelli, et al., GEANT4: A simulation toolkit, Nucl. Instrum. Meth. A 506 (2003) 250.
[14] M. Clemencic, et al., The LHCb simulation application, GAUSS: design, evolution and experience, J. Phys.: Conf. Ser. 331 (2011) 032023.
[15] A. Powell, et al., Particle identification at LHCb, PoS ICHEP2010 (2010) 020, LHCb-PROC-2011-008.
[16] Particle Data Group, J. Beringer, et al., Review of particle physics, Phys. Rev. D 86 (2012) 010001.
[17] W.D. Hulsbergen, Decay chain fitting with a Kalman filter, Nucl. Instrum. Meth. A 552 (2005) 566, arXiv:physics/0503191.
[18] M. Pivk, F.R. Le, Diberder, sPlot: a statistical tool to unfold data distributions, Nucl. Instrum. Meth. A 555 (2005) 356, arXiv:physics/0402083.
[19] LHCb Collaboration, R. Aaij, et al., Measurement of b-hadron masses, Phys. Lett. B 708 (2012) 241, arXiv:1112.4896.
[20] J.D. Jackson, Remarks on the phenomenological analysis on resonances, Nuovo Cimento 34 (1964) 1664.
[21] F. Selleri, Off-shell pion–pion scattering in the $T = J = 1$ state, Phys. Lett. 3 (1962) 76.
[22] BaBar Collaboration, B. Aubert, et al., Branching fraction and charge asymmetry measurements in $B \to J/\psi \pi^+ \pi^-$ decays, Phys. Rev. D 76 (2007) 031101, arXiv:0704.1266.
[23] LHCb Collaboration, R. Aaij, et al., First observation of $B^0_s \to J/\psi f_0(980)$ decays, Phys. Lett. B 698 (2011) 115, arXiv:1102.0206.

[24] LHCb Collaboration, R. Aaij, et al., Analysis of the resonant components in $\bar{B}_s^0 \to J/\psi\pi^+\pi^-$ decays, Phys. Rev. D 86 (2012) 052006, arXiv:1204.5643.

[25] B.S. Zou, D.V. Bugg, Is $f_0(975)$ a narrow resonance?, Phys. Rev. D 48 (1993) R3948.

[26] D.V. Bugg, Comments on the σ and κ, Phys. Lett. B 572 (2003) 1.

[27] BES Collaboration, M. Ablikim, et al., The σ pole in $J/\psi \to \omega\pi^+\pi^-$, Phys. Lett. B 598 (2004) 149, arXiv:hep-ex/0406038.

[28] LHCb Collaboration, R. Aaij, et al., Measurement of the b hadron production fractions in 7 TeV pp collisions, Phys. Rev. D 85 (2012) 032008, arXiv:1111.2357.

[29] A. Jaeger, et al., Measurement of the track finding efficiency, LHCb-PUB-2011-025.

[30] LHCb Collaboration, R. Aaij, et al., Measurement of relative branching fractions of B decays to $\psi(2S)$ and J/ψ mesons, Eur. Phys. J. C 72 (2012) 2118, arXiv:1205.0918.

[31] K. De Bruyn, et al., Branching ratio measurements of $B_{(s)}^0$ decays, Phys. Rev. D 86 (2012) 014027, arXiv:1204.1735.

LHCb Collaboration

R. Aaij [38], C. Abellan Beteta [33,n], A. Adametz [11], B. Adeva [34],
M. Adinolfi [43], C. Adrover [6], A. Affolder [49], Z. Ajaltouni [5], J. Albrecht [35],
F. Alessio [35], M. Alexander [48], S. Ali [38], G. Alkhazov [27],
P. Alvarez Cartelle [34], A.A. Alves Jr. [22], S. Amato [2], Y. Amhis [36],
L. Anderlini [17,f], J. Anderson [37], R.B. Appleby [51], O. Aquines Gutierrez [10],
F. Archilli [18,35], A. Artamonov [32], M. Artuso [53], E. Aslanides [6],
G. Auriemma [22,m], S. Bachmann [11], J.J. Back [45], C. Baesso [54],
V. Balagura [36,28], W. Baldini [16], R.J. Barlow [51], C. Barschel [35], S. Barsuk [7],
W. Barter [44], A. Bates [48], Th. Bauer [38], A. Bay [36], J. Beddow [48],
I. Bediaga [1], S. Belogurov [28], K. Belous [32], I. Belyaev [28,*], E. Ben-Haim [8],
M. Benayoun [8], G. Bencivenni [18], S. Benson [47], J. Benton [43],
A. Berezhnoy [29], R. Bernet [37], M.-O. Bettler [44], M. van Beuzekom [38],
A. Bien [11], S. Bifani [12], T. Bird [51], A. Bizzeti [17,h], P.M. Bjørnstad [51],
T. Blake [35], F. Blanc [36], C. Blanks [50], J. Blouw [11], S. Blusk [53], A. Bobrov [31],
V. Bocci [22], A. Bondar [31], N. Bondar [27], W. Bonivento [15], S. Borghi [48,51],
A. Borgia [53], T.J.V. Bowcock [49], C. Bozzi [16], T. Brambach [9],
J. van den Brand [39], J. Bressieux [36], D. Brett [51], M. Britsch [10], T. Britton [53],
N.H. Brook [43], H. Brown [49], A. Büchler-Germann [37], I. Burducea [26],
A. Bursche [37], J. Buytaert [35], S. Cadeddu [15], O. Callot [7], M. Calvi [20,j],
M. Calvo Gomez [33,n], A. Camboni [33], P. Campana [18,35], A. Carbone [14,c],
G. Carboni [21,k], R. Cardinale [19,i], A. Cardini [15], L. Carson [50],
K. Carvalho Akiba [2], G. Casse [49], M. Cattaneo [35], Ch. Cauet [9],
M. Charles [52], Ph. Charpentier [35], P. Chen [3,36], N. Chiapolini [37],
M. Chrzaszcz [23], K. Ciba [35], X. Cid Vidal [34], G. Ciezarek [50],
P.E.L. Clarke [47], M. Clemencic [35], H.V. Cliff [44], J. Closier [35], C. Coca [26],
V. Coco [38], J. Cogan [6], E. Cogneras [5], P. Collins [35],
A. Comerma-Montells [33], A. Contu [52,15], A. Cook [43], M. Coombes [43],

G. Corti [35], B. Couturier [35], G.A. Cowan [36], D. Craik [45], S. Cunliffe [50],
R. Currie [47], C. D'Ambrosio [35], P. David [8], P.N.Y. David [38], I. De Bonis [4],
K. De Bruyn [38], S. De Capua [21,k], M. De Cian [37], J.M. De Miranda [1],
L. De Paula [2], P. De Simone [18], D. Decamp [4], M. Deckenhoff [9],
H. Degaudenzi [36,35], L. Del Buono [8], C. Deplano [15], D. Derkach [14],
O. Deschamps [5], F. Dettori [39], J. Dickens [44], H. Dijkstra [35],
P. Diniz Batista [1], F. Domingo Bonal [33,n], S. Donleavy [49], F. Dordei [11],
A. Dosil Suárez [34], D. Dossett [45], A. Dovbnya [40], F. Dupertuis [36],
R. Dzhelyadin [32], A. Dziurda [23], A. Dzyuba [27], S. Easo [46], U. Egede [50],
V. Egorychev [28], S. Eidelman [31], D. van Eijk [38], F. Eisele [11],
S. Eisenhardt [47], R. Ekelhof [9], L. Eklund [48], I. El Rifai [5], Ch. Elsasser [37],
D. Elsby [42], D. Esperante Pereira [34], A. Falabella [14,e], C. Färber [11],
G. Fardell [47], C. Farinelli [38], S. Farry [12], V. Fave [36], V. Fernandez Albor [34],
F. Ferreira Rodrigues [1], M. Ferro-Luzzi [35], S. Filippov [30], C. Fitzpatrick [35],
M. Fontana [10], F. Fontanelli [19,i], R. Forty [35], O. Francisco [2], M. Frank [35],
C. Frei [35], M. Frosini [17,f], S. Furcas [20], A. Gallas Torreira [34], D. Galli [14,c],
M. Gandelman [2], P. Gandini [52], Y. Gao [3], J.-C. Garnier [35], J. Garofoli [53],
J. Garra Tico [44], L. Garrido [33], C. Gaspar [35], R. Gauld [52], E. Gersabeck [11],
M. Gersabeck [35], T. Gershon [45,35], Ph. Ghez [4], V. Gibson [44],
V.V. Gligorov [35], C. Göbel [54], D. Golubkov [28], A. Golutvin [50,28,35],
A. Gomes [2], H. Gordon [52], M. Grabalosa Gándara [33], R. Graciani Diaz [33],
L.A. Granado Cardoso [35], E. Graugés [33], G. Graziani [17], A. Grecu [26],
E. Greening [52], S. Gregson [44], O. Grünberg [55], B. Gui [53], E. Gushchin [30],
Yu. Guz [32], T. Gys [35], C. Hadjivasiliou [53], G. Haefeli [36], C. Haen [35],
S.C. Haines [44], S. Hall [50], T. Hampson [43], S. Hansmann-Menzemer [11],
N. Harnew [52], S.T. Harnew [43], J. Harrison [51], P.F. Harrison [45],
T. Hartmann [55], J. He [7], V. Heijne [38], K. Hennessy [49], P. Henrard [5],
J.A. Hernando Morata [34], E. van Herwijnen [35], E. Hicks [49], D. Hill [52],
M. Hoballah [5], P. Hopchev [4], W. Hulsbergen [38], P. Hunt [52], T. Huse [49],
N. Hussain [52], R.S. Huston [12], D. Hutchcroft [49], D. Hynds [48],
V. Iakovenko [41], P. Ilten [12], J. Imong [43], R. Jacobsson [35], A. Jaeger [11],
M. Jahjah Hussein [5], E. Jans [38], F. Jansen [38], P. Jaton [36], B. Jean-Marie [7],
F. Jing [3], M. John [52], D. Johnson [52], C.R. Jones [44], B. Jost [35], M. Kaballo [9],
S. Kandybei [40], M. Karacson [35], M. Karbach [35], J. Keaveney [12],
I.R. Kenyon [42], U. Kerzel [35], T. Ketel [39], A. Keune [36], B. Khanji [20],
Y.M. Kim [47], O. Kochebina [7], I. Komarov [29], V. Komarov [36],
R.F. Koopman [39], P. Koppenburg [38], M. Korolev [29], A. Kozlinskiy [38],

L. Kravchuk [30], K. Kreplin [11], M. Kreps [45], G. Krocker [11], P. Krokovny [31], F. Kruse [9], M. Kucharczyk [20,23,j], V. Kudryavtsev [31], T. Kvaratskheliya [28,35], V.N. La Thi [36], D. Lacarrere [35], G. Lafferty [51], A. Lai [15], D. Lambert [47], R.W. Lambert [39], E. Lanciotti [35], G. Lanfranchi [18,35], C. Langenbruch [35], T. Latham [45], C. Lazzeroni [42], R. Le Gac [6], J. van Leerdam [38], J.-P. Lees [4], R. Lefèvre [5], A. Leflat [29,35], J. Lefrançois [7], O. Leroy [6], T. Lesiak [23], L. Li [3], Y. Li [3], L. Li Gioi [5], M. Liles [49], R. Lindner [35], C. Linn [11], B. Liu [3], G. Liu [35], J. von Loeben [20], J.H. Lopes [2], E. Lopez Asamar [33], N. Lopez-March [36], H. Lu [3], J. Luisier [36], A. Mac Raighne [48], F. Machefert [7], I.V. Machikhiliyan [4,28], F. Maciuc [26], O. Maev [27,35], J. Magnin [1], M. Maino [20], S. Malde [52], G. Manca [15,d], G. Mancinelli [6], N. Mangiafave [44], U. Marconi [14], R. Märki [36], J. Marks [11], G. Martellotti [22], A. Martens [8], L. Martin [52], A. Martín Sánchez [7], M. Martinelli [38], D. Martinez Santos [35], A. Massafferri [1], Z. Mathe [35], C. Matteuzzi [20], M. Matveev [27], E. Maurice [6], A. Mazurov [16,30,35], J. McCarthy [42], G. McGregor [51], R. McNulty [12], M. Meissner [11], M. Merk [38], J. Merkel [9], D.A. Milanes [13], M.-N. Minard [4], J. Molina Rodriguez [54], S. Monteil [5], D. Moran [51], P. Morawski [23], R. Mountain [53], I. Mous [38], F. Muheim [47], K. Müller [37], R. Muresan [26], B. Muryn [24], B. Muster [36], J. Mylroie-Smith [49], P. Naik [43], T. Nakada [36], R. Nandakumar [46], I. Nasteva [1], M. Needham [47], N. Neufeld [35], A.D. Nguyen [36], C. Nguyen-Mau [36,o], M. Nicol [7], V. Niess [5], N. Nikitin [29], T. Nikodem [11], A. Nomerotski [52,35], A. Novoselov [32], A. Oblakowska-Mucha [24], V. Obraztsov [32], S. Oggero [38], S. Ogilvy [48], O. Okhrimenko [41], R. Oldeman [15,35,d], M. Orlandea [26], J.M. Otalora Goicochea [2], P. Owen [50], B.K. Pal [53], A. Palano [13,b], M. Palutan [18], J. Panman [35], A. Papanestis [46], M. Pappagallo [48], C. Parkes [51], C.J. Parkinson [50], G. Passaleva [17], G.D. Patel [49], M. Patel [50], G.N. Patrick [46], C. Patrignani [19,i], C. Pavel-Nicorescu [26], A. Pazos Alvarez [34], A. Pellegrino [38], G. Penso [22,l], M. Pepe Altarelli [35], S. Perazzini [14,c], D.L. Perego [20,j], E. Perez Trigo [34], A. Pérez-Calero Yzquierdo [33], P. Perret [5], M. Perrin-Terrin [6], G. Pessina [20], K. Petridis [50], A. Petrolini [19,i], A. Phan [53], E. Picatoste Olloqui [33], B. Pie Valls [33], B. Pietrzyk [4], T. Pilař [45], D. Pinci [22], S. Playfer [47], M. Plo Casasus [34], F. Polci [8], G. Polok [23], A. Poluektov [45,31], E. Polycarpo [2], D. Popov [10], B. Popovici [26], C. Potterat [33], A. Powell [52], J. Prisciandaro [36], V. Pugatch [41], A. Puig Navarro [36], W. Qian [3], J.H. Rademacker [43], B. Rakotomiaramanana [36], M.S. Rangel [2],

I. Raniuk [40], N. Rauschmayr [35], G. Raven [39], S. Redford [52], M.M. Reid [45],
A.C. dos Reis [1], S. Ricciardi [46], A. Richards [50], K. Rinnert [49],
V. Rives Molina [33], D.A. Roa Romero [5], P. Robbe [7], E. Rodrigues [48,51],
P. Rodriguez Perez [34], G.J. Rogers [44], S. Roiser [35], V. Romanovsky [32],
A. Romero Vidal [34], J. Rouvinet [36], T. Ruf [35], H. Ruiz [33], G. Sabatino [21,k],
J.J. Saborido Silva [34], N. Sagidova [27], P. Sail [48], B. Saitta [15,d],
C. Salzmann [37], B. Sanmartin Sedes [34], M. Sannino [19,i], R. Santacesaria [22],
C. Santamarina Rios [34], R. Santinelli [35], E. Santovetti [21,k], M. Sapunov [6],
A. Sarti [18,l], C. Satriano [22,m], A. Satta [21], M. Savrie [16,e], D. Savrina [28],
P. Schaack [50], M. Schiller [39], H. Schindler [35], S. Schleich [9], M. Schlupp [9],
M. Schmelling [10], B. Schmidt [35], O. Schneider [36], A. Schopper [35],
M.-H. Schune [7], R. Schwemmer [35], B. Sciascia [18], A. Sciubba [18,l],
M. Seco [34], A. Semennikov [28], K. Senderowska [24], I. Sepp [50], N. Serra [37],
J. Serrano [6], P. Seyfert [11], M. Shapkin [32], I. Shapoval [40,35], P. Shatalov [28],
Y. Shcheglov [27], T. Shears [49,35], L. Shekhtman [31], O. Shevchenko [40],
V. Shevchenko [28], A. Shires [50], R. Silva Coutinho [45], T. Skwarnicki [53],
N.A. Smith [49], E. Smith [52,46], M. Smith [51], K. Sobczak [5], F.J.P. Soler [48],
A. Solomin [43], F. Soomro [18,35], D. Souza [43], B. Souza De Paula [2],
B. Spaan [9], A. Sparkes [47], P. Spradlin [48], F. Stagni [35], S. Stahl [11],
O. Steinkamp [37], S. Stoica [26], S. Stone [53], B. Storaci [38], M. Straticiuc [26],
U. Straumann [37], V.K. Subbiah [35], S. Swientek [9], M. Szczekowski [25],
P. Szczypka [36,35], T. Szumlak [24], S. T'Jampens [4], M. Teklishyn [7],
E. Teodorescu [26], F. Teubert [35], C. Thomas [52], E. Thomas [35],
J. van Tilburg [11], V. Tisserand [4], M. Tobin [37], S. Tolk [39],
S. Topp-Joergensen [52], N. Torr [52], E. Tournefier [4,50], S. Tourneur [36],
M.T. Tran [36], A. Tsaregorodtsev [6], N. Tuning [38], M. Ubeda Garcia [35],
A. Ukleja [25], D. Urner [51], U. Uwer [11], V. Vagnoni [14], G. Valenti [14],
R. Vazquez Gomez [33], P. Vazquez Regueiro [34], S. Vecchi [16], J.J. Velthuis [43],
M. Veltri [17,g], G. Veneziano [36], M. Vesterinen [35], B. Viaud [7], I. Videau [7],
D. Vieira [2], X. Vilasis-Cardona [33,n], J. Visniakov [34], A. Vollhardt [37],
D. Volyanskyy [10], D. Voong [43], A. Vorobyev [27], V. Vorobyev [31], H. Voss [10],
C. Voß [55], R. Waldi [55], R. Wallace [12], S. Wandernoth [11], J. Wang [53],
D.R. Ward [44], N.K. Watson [42], A.D. Webber [51], D. Websdale [50],
M. Whitehead [45], J. Wicht [35], D. Wiedner [11], L. Wiggers [38],
G. Wilkinson [52], M.P. Williams [45,46], M. Williams [50,p], F.F. Wilson [46],
J. Wishahi [9], M. Witek [23,35], W. Witzeling [35], S.A. Wotton [44], S. Wright [44],
S. Wu [3], K. Wyllie [35], Y. Xie [47], F. Xing [52], Z. Xing [53], Z. Yang [3],

R. Young [47], X. Yuan [3], O. Yushchenko [32], M. Zangoli [14],
M. Zavertyaev [10,a], F. Zhang [3], L. Zhang [53], W.C. Zhang [12], Y. Zhang [3],
A. Zhelezov [11], L. Zhong [3], A. Zvyagin [35]

[1] *Centro Brasileiro de Pesquisas Físicas (CBPF), Rio de Janeiro, Brazil*
[2] *Universidade Federal do Rio de Janeiro (UFRJ), Rio de Janeiro, Brazil*
[3] *Center for High Energy Physics, Tsinghua University, Beijing, China*
[4] *LAPP, Université de Savoie, CNRS/IN2P3, Annecy-Le-Vieux, France*
[5] *Clermont Université, Université Blaise Pascal, CNRS/IN2P3, LPC, Clermont-Ferrand, France*
[6] *CPPM, Aix-Marseille Université, CNRS/IN2P3, Marseille, France*
[7] *LAL, Université Paris-Sud, CNRS/IN2P3, Orsay, France*
[8] *LPNHE, Université Pierre et Marie Curie, Université Paris Diderot, CNRS/IN2P3, Paris, France*
[9] *Fakultät Physik, Technische Universität Dortmund, Dortmund, Germany*
[10] *Max-Planck-Institut für Kernphysik (MPIK), Heidelberg, Germany*
[11] *Physikalisches Institut, Ruprecht-Karls-Universität Heidelberg, Heidelberg, Germany*
[12] *School of Physics, University College Dublin, Dublin, Ireland*
[13] *Sezione INFN di Bari, Bari, Italy*
[14] *Sezione INFN di Bologna, Bologna, Italy*
[15] *Sezione INFN di Cagliari, Cagliari, Italy*
[16] *Sezione INFN di Ferrara, Ferrara, Italy*
[17] *Sezione INFN di Firenze, Firenze, Italy*
[18] *Laboratori Nazionali dell'INFN di Frascati, Frascati, Italy*
[19] *Sezione INFN di Genova, Genova, Italy*
[20] *Sezione INFN di Milano Bicocca, Milano, Italy*
[21] *Sezione INFN di Roma Tor Vergata, Roma, Italy*
[22] *Sezione INFN di Roma La Sapienza, Roma, Italy*
[23] *Henryk Niewodniczanski Institute of Nuclear Physics Polish Academy of Sciences, Kraków, Poland*
[24] *AGH University of Science and Technology, Kraków, Poland*
[25] *National Center for Nuclear Research (NCBJ), Warsaw, Poland*
[26] *Horia Hulubei National Institute of Physics and Nuclear Engineering, Bucharest-Magurele, Romania*
[27] *Petersburg Nuclear Physics Institute (PNPI), Gatchina, Russia*
[28] *Institute of Theoretical and Experimental Physics (ITEP), Moscow, Russia*
[29] *Institute of Nuclear Physics, Moscow State University (SINP MSU), Moscow, Russia*
[30] *Institute for Nuclear Research of the Russian Academy of Sciences (INR RAN), Moscow, Russia*
[31] *Budker Institute of Nuclear Physics (SB RAS) and Novosibirsk State University, Novosibirsk, Russia*
[32] *Institute for High Energy Physics (IHEP), Protvino, Russia*
[33] *Universitat de Barcelona, Barcelona, Spain*
[34] *Universidad de Santiago de Compostela, Santiago de Compostela, Spain*
[35] *European Organization for Nuclear Research (CERN), Geneva, Switzerland*
[36] *Ecole Polytechnique Fédérale de Lausanne (EPFL), Lausanne, Switzerland*
[37] *Physik-Institut, Universität Zürich, Zürich, Switzerland*
[38] *Nikhef National Institute for Subatomic Physics, Amsterdam, The Netherlands*
[39] *Nikhef National Institute for Subatomic Physics and VU University Amsterdam, Amsterdam, The Netherlands*
[40] *NSC Kharkiv Institute of Physics and Technology (NSC KIPT), Kharkiv, Ukraine*
[41] *Institute for Nuclear Research of the National Academy of Sciences (KINR), Kyiv, Ukraine*
[42] *University of Birmingham, Birmingham, United Kingdom*
[43] *H.H. Wills Physics Laboratory, University of Bristol, Bristol, United Kingdom*
[44] *Cavendish Laboratory, University of Cambridge, Cambridge, United Kingdom*
[45] *Department of Physics, University of Warwick, Coventry, United Kingdom*
[46] *STFC Rutherford Appleton Laboratory, Didcot, United Kingdom*
[47] *School of Physics and Astronomy, University of Edinburgh, Edinburgh, United Kingdom*
[48] *School of Physics and Astronomy, University of Glasgow, Glasgow, United Kingdom*
[49] *Oliver Lodge Laboratory, University of Liverpool, Liverpool, United Kingdom*
[50] *Imperial College London, London, United Kingdom*
[51] *School of Physics and Astronomy, University of Manchester, Manchester, United Kingdom*

[52] *Department of Physics, University of Oxford, Oxford, United Kingdom*
[53] *Syracuse University, Syracuse, NY, United States*
[54] *Pontifícia Universidade Católica do Rio de Janeiro (PUC-Rio), Rio de Janeiro, Brazil [b]*
[55] *Institut für Physik, Universität Rostock, Rostock, Germany [k]*

[*] Corresponding author.
  E-mail address: Ivan.Belyaev@cern.ch (I. Belyaev).
[a] P.N. Lebedev Physical Institute, Russian Academy of Science (LPI RAS), Moscow, Russia.
[b] Università di Bari, Bari, Italy.
[c] Università di Bologna, Bologna, Italy.
[d] Università di Cagliari, Cagliari, Italy.
[e] Università di Ferrara, Ferrara, Italy.
[f] Università di Firenze, Firenze, Italy.
[g] Università di Urbino, Urbino, Italy.
[h] Università di Modena e Reggio Emilia, Modena, Italy.
[i] Università di Genova, Genova, Italy.
[j] Università di Milano Bicocca, Milano, Italy.
[k] Università di Roma Tor Vergata, Roma, Italy.
[l] Università di Roma La Sapienza, Roma, Italy.
[m] Università della Basilicata, Potenza, Italy.
[n] LIFAELS, La Salle, Universitat Ramon Llull, Barcelona, Spain.
[o] Hanoi University of Science, Hanoi, Vietnam.
[p] Massachusetts Institute of Technology, Cambridge, MA, United States.